Eur. J. Mech. B - Fluids 19 (2000) 469–490

S0997-7546(00)00128-X/FLA

Algebraic growth in boundary layers: optimal control by blowing and suction at the wall

Patricia Cathalifaud [a], Paolo Luchini [b,*]

[a] *Institut de Mécanique des Fluides de Toulouse, Université Paul Sabatier, 118 route de Narbonne, 31062 Toulouse, France*
[b] *Dipartimento di Ingegneria Aerospaziale, Politecnico di Milano, via La Masa 34, 20158 Milano, Italy*

(Received 8 May 1999; revised and accepted 22 March 2000)

Abstract – The upstream perturbations that maximise the spatial energy growth in a boundary layer are called optimal perturbations. The optimal perturbations correspond to streamwise vortices and the downstream response corresponds to streamwise streaks.

The aim of the present paper is to find a control by blowing and suction at the wall that zeros the energy of perturbation, when the initial disturbance is itself optimal. We shall also address the question: which kind of blowing and suction at the wall is most effective in controlling optimal disturbances?

The problem is examined by a method of receptivity analysis based on a numerical solution of a system of equations adjoint to the linearised boundary layer equations. We shall investigate both cases of a flat and a concave wall. © 2000 Éditions scientifiques et médicales Elsevier SAS

1. Introduction

Landahl [1] has shown that an inviscid shear flow is unstable for a wide class of three-dimensional infinitesimal disturbances, and that the disturbance energy increases at least linearly with time. This is the 'lift-up' effect. On taking the viscous damping into account, we get the phenomenon of transient growth or algebraic instability. This subject is dealt with, e.g., in the works of Hultgren and Gustavsson [2], Gustavsson [3], Butler and Farrell [4], Henningson et al. [5], Reddy and Henningson [6], Trefethen et al. [7] and Luchini [8]. These studies have built a theoretical model which enables us to describe the early transition of the boundary layer observed in some experiments.

For a given definition of disturbance energy, we can calculate the input disturbance of the boundary layer that maximises the output disturbance energy, i.e. the optimal perturbation. For the spatial algebraic growth of steady disturbances leading to bypass transition in the boundary layer over a flat surface, this 'optimal' input disturbance was calculated by Luchini [9] and Andersson et al. [10,11]. They found that this optimal upstream disturbance comes in the form of stationary streamwise vortices, whereas the velocity field it induces is dominated by streamwise streaks. Indeed, streamwise streaks have long been known to appear in laminar and transitional boundary layers, and are generally assumed to play a part in the transition to turbulence. Klebanoff et al. [12] identified them in experiments; that is why we sometimes call these streamwise streaks Klebanoff modes.

Many flows exhibit the following scenario: the flow starts out in a laminar state which is unstable; then a linear instability develops, and grows up to the point where nonlinear interactions finally lead to turbulence. In many applications, it might be very interesting to delay this transition towards turbulence and thus to maintain

* Correspondence and reprints; e-mail: luchini@aero.polimi.it

the flow laminar. Consequently, one of the first objectives, within this framework, of a system of flow control will be to control these instabilities. In this paper, our aim is to control the streamwise vortices which may lead the boundary layer towards the transition to turbulence.

Stationary streamwise vortices are encountered in at least three different situations. First, in the boundary layer over a concave wall, competition between centrifugal and pressure forces creates an instability leading to Görtler vortices (cf. Görtler [13], Hall [14,15], Floryan and Saric [16], Swearingen and Blackwelder [17], Peerhossaini and Wesfreid [18], Sabry and Liu [19], Saric [20], Bottaro and Klingmann [21]). This instability comes in the form of steady counter-rotating streamwise vortices, periodic in the transverse direction. The second type of streamwise vortices is found in the laminar or transitional boundary layer over a flat plate (Klebanoff et al. [12]): they come from small variations of the upstream main flow (low turbulence noise) (Kendall [22]), from the imperfections of the wall, or, as Anders and Blackwelder [23] have shown in their experiments, from the wind tunnel screens of the convergent. The last type of streamwise vortices is found in fully developed turbulence. However, these vortices appear randomly and are much more short-lived than the two previous types.

It appears from the literature that a dynamic control by blowing and suction would be the most convenient mean for controlling a boundary-layer flow (Floryan and Saric [24], Myose and Blackwelder [25,26]). Assuming that an optimal initial perturbation is present, in this paper we shall seek to determine the control by blowing and suction at the wall that most effectively counteracts such a perturbation.

The framework of our study is ‘optimal’ control. In the treatment of this control problem, we shall use a ‘backward-in-time’ approach, i.e. an upstream integration of adjoint equations. The application to fluid dynamic instabilities of this method was initiated by Hill [27], who pointed out the role of adjoint systems in the local receptivity problem for a boundary layer, and developed for nonlocal Görtler instabilities by Luchini and Bottaro [28], who thus provided the computational framework for the works of Luchini [9] and Andersson et al. [10,11]. The mathematical theory of optimal control is described, for example, by Gunzburger [29] and Borggaard et al. [30]. The principle of optimal control is the minimisation of a given ‘objective functional’. Thus, this approach does not need any a priori knowledge of the characteristics of the disturbance to be controlled, and can be applied to many types of flow (cf. Bewley et al. [31,32] and Gunzburger and Hou [33] in connection with the nonlinear problems, and Abergel and Teman [34], Moin and Bewley [35], Temam et al. [36] for problems more particularly related to the the control of turbulence).

In practice, for a given controlling input, we choose an objective functional to be minimised, and by a formal minimisation procedure we obtain a system of differential equations (state equations and adjoint equations) and conditions of optimality, whose solution gives the optimal control. The results can then be applied to develop mechanisms for either passive or active control. This approach was used in particular by Joslin et al. [37] to control the evolution of TS waves in a flat-plate boundary layer, and by Joshi et al. [38] in the case of Poiseuille flow. Also in the case of plane Poiseuille flow, Bewley and Liu [39] tested the effectiveness of optimal control on the linearly unstable disturbances (by including free stream turbulence).

This paper is organised as follows. In section 2, the method of adjoint equations is presented. In section 3, the numerical determination of an optimal control by blowing and suction is described. In section 4, the results are presented and discussed.

2. The method of adjoint equations

We shall first describe the governing equations of the direct problem, and then present the adjoint problem.

We qualify the perturbation studied here as Reynolds-number independent (for a justification and discussion of this concept, the reader is referred to Luchini [8,9]). Since the type of control chosen is a control by blowing and suction at the wall, the wall-normal velocity of perturbation v is imposed to be different from zero at the plate surface. So, we have $v(x,0) = V_w(x)$, where $V_w(x)$ is the velocity of blowing (or suction) at the wall.

2.1. Direct problem

We describe our problem by means of the linearised, steady, three-dimensional boundary layer equations (see, e.g., Luchini and Bottaro [28]), whose solution is assumed to be sinusoidally varying in z as $\exp(-i\beta z)$. They read

$$\begin{aligned} (Uw)_x + (Vw)_y - i\beta p &= w_{yy} - \beta^2 w, \\ (Vu + Uv)_x + (2Vv)_y - i\beta Vw + 2G^2 Uu + p_y &= v_{yy} - \beta^2 v, \\ (Uu)_x + Vu_y + U_y v &= u_{yy} - \beta^2 u, \\ u_x + v_y - i\beta w &= 0, \end{aligned} \tag{1}$$

with the boundary conditions

$$u(x,0) = w(x,0) = 0, \qquad v(x,0) = V_w(x), \quad \text{and} \quad u(x,\infty) = w(x,\infty) = p(x,\infty) = 0. \tag{2}$$

Here x is the longitudinal coordinate, y the wall-normal coordinate, and z the spanwise coordinate.

According to boundary-layer scaling, x is made dimensionless with respect to a reference length L, and y and z with respect to $\delta = Re^{-1/2}L$. The longitudinal velocities, U for the base flow and u for the perturbation, are made dimensionless with respect to the free-stream velocity U_∞, whereas the wall-normal and spanwise velocities with respect to $Re^{-1/2}U_\infty$. The Reynolds number is defined as $Re = U_\infty L/\nu$. G represents a nondimensionalised curvature of the wall, of radius $\mathcal{R}$, according to the definition $G^2 = Re^{1/2}L/\mathcal{R}$. It is one of the possible definitions for the Görtler number, and $G = 0$ corresponds to a flat plate.

Following Luchini [9], we introduce a modified longitudinal vorticity perturbation, according to the definition:

$$\eta = (Uw)_y + i\beta(Uv + Vu). \tag{3}$$

The system of equations (1) is parabolic in x, so that its solution is completely determined by an initial condition at $x = x_{\text{in}}$ of the form:

$$u(x_{\text{in}}, y) = u_{\text{in}}(y) \quad \text{and} \quad \eta(x_{\text{in}}, y) = \eta_{\text{in}}(y). \tag{4}$$

In fact, only two conditions are necessary to form a well posed problem (cf. Luchini and Bottaro [28]). By introducing the vector $\vec{q} = (w, p, u, v)^T$, and the two matrices $\underline{\underline{A}}$ and $\underline{\underline{B}}$, given by

$$\underline{\underline{A}} = \begin{pmatrix} V_y + V\frac{\partial}{\partial y} - \frac{\partial^2}{\partial y^2} + \beta^2 & -i\beta & 0 & 0 \\ -Vi\beta & \frac{\partial}{\partial y} & 2G^2U & 2V_y + 2V\frac{\partial}{\partial y} - \frac{\partial^2}{\partial y^2} + \beta^2 \\ 0 & 0 & V\frac{\partial}{\partial y} - \frac{\partial^2}{\partial y^2} + \beta^2 & U_y \\ -i\beta & 0 & 0 & \frac{\partial}{\partial y} \end{pmatrix}$$

and

$$\underline{\underline{B}} = \begin{pmatrix} U & 0 & 0 & 0 \\ 0 & 0 & V & U \\ 0 & 0 & U & 0 \\ 0 & 0 & 1 & 0 \end{pmatrix},$$

system (1) may be compactly written as

$$\left(\underline{\underline{B}} \cdot \vec{q}\right)_x + \underline{\underline{A}} \cdot \vec{q} = 0, \tag{5}$$

with boundary conditions (2) and initial conditions (4). We shall also need the boundary vector $\vec{q}_w = (0,\, p(x,0),\, 0,\, V_w(x))$.

The system (5) has been discretised by second-order central differences in y, on a regular unevenly-spaced mesh in which w and p are staggered by half a step with respect to u and v. If first-order backward differences are adopted in the x-direction, the resulting system can be expressed as

$$\left(\underline{\underline{A_n}} + \frac{1}{\Delta x}\underline{\underline{B_n}}\right) \cdot \vec{q}_n + \underline{\underline{C_n}} \cdot \vec{q}_{w_n} = \frac{1}{\Delta x}\underline{\underline{B_{n-1}}} \cdot \vec{q}_{n-1}. \tag{6}$$

If, instead, second-order backward differences are adopted,

$$\left(\underline{\underline{A_n}} + \frac{1.5}{\Delta x}\underline{\underline{B_n}}\right) \cdot \vec{q}_n + \underline{\underline{C_n}} \cdot \vec{q}_{w_n} = \frac{2}{\Delta x}\underline{\underline{B_{n-1}}} \cdot \vec{q}_{n-1} - \frac{0.5}{\Delta x}\underline{\underline{B_{n-2}}} \cdot \vec{q}_{n-2}. \tag{7}$$

The boundary conditions are included in the appropriate rows of matrix $\underline{\underline{A}}$; the control forcing, represented by an imposed nonzero value of the normal velocity v at the wall, appears in the term $\underline{\underline{C}} \cdot \vec{q}_w = (0, 0, 0, V_w(x))$.

Once the initial conditions (4) are imposed, equations (6) or (7) must be iterated forward, from the initial position, $x = x_{\text{in}}$, to the final position, $x = x_{\text{out}}$, to calculate the output perturbation produced by a given initial perturbation and wall forcing.

In this paper, we shall use $x_{\text{in}} = 0^-$ and $x_{\text{out}} = 1$, i.e. we shall assume that the initial perturbation comes from upstream of the leading edge and that the total length of the plate has been assumed as the reference length L. So, the forward iteration begins at $n = 0$ and ends at $n = N$ (with $N\ \Delta x = 1$).

2.2. Adjoint problem

The procedure for obtaining the adjoint equations from the direct problem is the same as the one used by Luchini and Bottaro [28]. Let $\vec{\xi} = (d(x,y), c(x,y), b(x,y), a(x,y))$ be the vector of the receptivity coefficients (adjoint variables). Taking the scalar product of the vector $\vec{\xi}$ with equations (5), integrating in y, and applying integration by parts yields

$$\begin{aligned}
&\frac{\mathrm{d}}{\mathrm{d}x}\int_0^\infty \left(au + bUu + c(Vu + Uv) + dUw\right)\mathrm{d}y \\
&\quad + \left[av + bVu - bu_y + b_y u + cp + 2cVv - cv_y + c_y v + dVw - dw_y + d_y w\right]_0^\infty \\
&\quad + \int_0^\infty -u\left(a_x + Ub_x + Vc_x + (Vb)_y + b_{yy} - \beta^2 b - 2G^2 Uc\right)\mathrm{d}y \\
&\quad + \int_0^\infty -v\left(Uc_x + a_y + 2Vc_y + c_{yy} - U_y b - \beta^2 c\right)\mathrm{d}y
\end{aligned}$$

$$+\int_0^\infty -w\left(Ud_x+Vd_y+d_{yy}+i\beta a+i\beta Vc-\beta^2 d\right)\mathrm{d}y+\int_0^\infty -p(c_y+i\beta d)\,\mathrm{d}y=0. \tag{8}$$

We choose $\vec{\xi}$ in such a way that

$$\begin{aligned} a_x+Ub_x+Vc_x+(Vb)_y+b_{yy}-\beta^2 b &= 2G^2Uc,\\ Uc_x+2Vc_y+c_{yy}-\beta^2 c &= U_y b-a_y,\\ Ud_x+Vd_y+d_{yy}-\beta^2 d &= -i\beta(a+Vc),\\ c_y &= -i\beta d \end{aligned} \tag{9}$$

with boundary conditions

$$b=c=d=0 \quad \text{at } y=0 \quad \text{and} \quad a+2Vc+c_y=0 \quad \text{for } y\to\infty. \tag{10}$$

The adjoint system (9), the boundary conditions (10), and the equations (8) are such that the scalar product

$$s=\langle\vec{\xi},\underline{\underline{B}}\vec{q}\rangle=\int_0^\infty (au+bUu+c(Vu+Uv)+dUw)\,\mathrm{d}y \tag{11}$$

satisfies

$$\frac{\mathrm{d}s}{\mathrm{d}x}=(a(x,0)+c_y(x,0))V_w(x). \tag{12}$$

The scalar product defined in the equation (11) can also be written, after a further integration by parts, as

$$s=\int_0^\infty (\overline{u}u+\overline{\eta}\eta)\,\mathrm{d}y, \tag{13}$$

thus defining the streak receptivity $\overline{u}(x,y)$ and the roll receptivity $\overline{\eta}(x,y)$ (cf. Luchini and Bottaro [28]). The discretisation of the backward system (9) is performed by taking the discrete adjoint of the forward discretisations (6) or (7). At first order, we define the discretised receptivity $\vec{\xi}_n$ through the scalar product

$$s_n=\vec{\xi}_n\cdot\underline{\underline{B_n}}\cdot\vec{q}_n \tag{14}$$

which, on using equation (6), yields

$$\begin{aligned} s_n-s_{n-1}=&\left[\frac{1}{\Delta x}\vec{\xi}_n\cdot\underline{\underline{B_n}}\cdot\left(\underline{\underline{A_n}}+\frac{1}{\Delta x}\underline{\underline{B_n}}\right)^{-1}-\vec{\xi}_{n-1}\right]\cdot\underline{\underline{B_{n-1}}}\cdot\vec{q}_{n-1}\\ &-\vec{\xi}_n\cdot\underline{\underline{B_n}}\cdot\left(\underline{\underline{A_n}}+\frac{1}{\Delta x}\underline{\underline{B_n}}\right)^{-1}\cdot\underline{\underline{C_n}}\cdot\vec{q}_{wn}. \end{aligned} \tag{15}$$

It follows that

$$\begin{aligned} \vec{\xi}_{n-1} &= \frac{1}{\Delta x}\vec{\xi}_n\cdot\underline{\underline{B_n}}\cdot\left(\underline{\underline{A_n}}+\frac{1}{\Delta x}\underline{\underline{B_n}}\right)^{-1},\\ s_n-s_{n-1} &= -\vec{\xi}_n\cdot\underline{\underline{B_n}}\cdot\left(\underline{\underline{A_n}}+\frac{1}{\Delta x}\underline{\underline{B_n}}\right)^{-1}\cdot\underline{\underline{C_n}}\cdot\vec{q}_{wn}. \end{aligned} \tag{16}$$

At second order we need two vectors $\vec{\xi}_n$ and $\vec{\xi}_n^{(1)}$ which weigh two successive levels of the discrete solution, and correspondingly define the discrete scalar product as

$$s_n = \vec{\xi}_n \cdot \underline{\underline{B_n}} \cdot \vec{q}_n + \vec{\xi}_n^{(1)} \cdot \left(\underline{\underline{B_n}} \cdot \vec{q}_n - \underline{\underline{B_{n-1}}} \cdot \vec{q}_{n-1}\right). \tag{17}$$

By a procedure similar to the previous one, we find that

$$\begin{aligned}
\vec{\xi}_{n-1}^{(1)} &= \frac{0.5}{\Delta x}\left(\vec{\xi}_n + \vec{\xi}_n^{(1)}\right) \cdot \underline{\underline{B_n}} \cdot \left(\underline{\underline{A_n}} + \frac{1.5}{\Delta x}\underline{\underline{B_n}}\right)^{-1}, \\
\vec{\xi}_{n-1} &= \frac{1.5}{\Delta x}\left(\vec{\xi}_n + \vec{\xi}_n^{(1)}\right) \cdot \underline{\underline{B_n}} \cdot \left(\underline{\underline{A_n}} + \frac{1.5}{\Delta x}\underline{\underline{B_n}}\right)^{-1} - \vec{\xi}_n^{(1)}, \\
s_n - s_{n-1} &= -\left(\vec{\xi}_n + \vec{\xi}_n^{(1)}\right) \cdot \underline{\underline{B_n}} \cdot \left(\underline{\underline{A_n}} + \frac{1.5}{\Delta x}\underline{\underline{B_n}}\right)^{-1} \cdot \underline{\underline{C_n}} \cdot \vec{q}_{w_n}.
\end{aligned} \tag{18}$$

The discretised adjoint problem is thus uniquely determined from the discretised forward problem. It will be iterated backward (from the outlet to the inlet section). The boundary conditions are automatically taken care of, provided that they were previously inserted in the appropriate rows of matrices $\underline{\underline{A}}$ and $\underline{\underline{B}}$.

We now describe why and how we can use these direct and adjoint systems to determine the optimal control of the optimal perturbation of the boundary layer.

3. Numerical determination of an optimal control by blowing and suction at the wall

3.1. Optimal control: method

The basic idea of the method of optimal control is the minimisation of a 'cost' (or 'objective') functional, which represents the physical quantity that we want to keep under control. We describe here, in a very general way, the classical method of optimisation based on Lagrange multipliers (cf. Gunzburger [40]).

Let u be the state variable, and c the control variable. We suppose that u and c obey the following problem

$$\vec{F}(u, c) = 0, \tag{19}$$

where $\vec{F} = (F_u, F_c)$. This relation (19) is called constraint equation, direct problem or state system. F_u is the constraint related to the state variable u, and F_c the one related to the control variable c. Then, we define a cost functional, $\mathcal{J}(u, c)$, which represents the objective to be minimised. It can, for example, be the energy of a disturbance, or a viscous drag. Often the cost of the control itself is included (via a weighing parameter) in this objective functional. The problem that consists in seeking u and c verifying the constraints (19) and such that the cost functional $\mathcal{J}(u, c)$ is minimal, is called a 'minimisation problem'.

A general approach to minimisation is to impose the previously defined constraints through a vector of Lagrange multipliers (which will turn out to be the same as the adjoint variables) $\vec{\xi} = (\xi_u, \xi_c)$. The lagrangian functional is thus defined as

$$\mathcal{L}\left(u, c, \vec{\xi}\,\right) = \mathcal{J}(u, c) - \left\langle \vec{F}(u, c), \vec{\xi}\,\right\rangle, \tag{20}$$

where $\langle \cdot, \cdot \rangle$ denotes a scalar product between the spaces of the state variables (u, c) and of the adjoint variables (ξ_u, ξ_c). For example $\langle \vec{F}(u, c), \vec{\xi}\,\rangle = \vec{F}(u, c)\ \vec{\xi}^*$, where * indicates complex conjugation. The optimisation

problem thus becomes one of seeking u, c and $\vec{\xi}$ such that $\mathcal{L}(u, c, \vec{\xi})$ is stationary, and leads to the following system:

$$\begin{cases} \dfrac{\partial \mathcal{L}}{\partial \xi_u} = \dfrac{\partial \mathcal{L}}{\partial \xi_c} = 0 \;\Rightarrow\; \text{constraint equations}, \\ \dfrac{\partial \mathcal{L}}{\partial c} = 0 \;\Rightarrow\; \text{optimality conditions}, \\ \dfrac{\partial \mathcal{L}}{\partial u} = 0 \;\Rightarrow\; \text{adjoint equations}. \end{cases} \tag{21}$$

It is fairly obvious that we recover the original constraint equations from the first relation of this system (21), which we shall call system of optimality. The adjoint system is formally written as

$$\frac{\partial \mathcal{J}}{\partial u} = \frac{\partial \vec{F}}{\partial u}\vec{\xi}^*, \tag{22}$$

and turns out to be the same as defined in the previous section. The optimality condition reads

$$\frac{\partial \mathcal{J}}{\partial c} = \frac{\partial \vec{F}}{\partial c}\vec{\xi}^*. \tag{23}$$

In practice this system of optimality is often solved by an iterative method, which implies calculating the gradient of the cost functional with respect to the control variable, $\mathrm{d}\mathcal{J}/\mathrm{d}c$. Indeed, the optimal control is the control that minimises $\mathcal{J}$, i.e. that nullifies $\mathrm{d}\mathcal{J}/\mathrm{d}c$, where

$$\mathrm{d}\mathcal{J}/\mathrm{d}c = \frac{\partial \mathcal{J}}{\partial u}\frac{\mathrm{d}u}{\mathrm{d}c} + \frac{\partial \mathcal{J}}{\partial c}. \tag{24}$$

Let $\vec{\xi}$ be the solution of the adjoint system. By using $\vec{\xi}$ and the fact that $\frac{\partial \vec{F}}{\partial u}\frac{\mathrm{d}u}{\mathrm{d}c} = -\frac{\partial \vec{F}}{\partial c}$, we obtain that

$$\frac{\mathrm{d}\mathcal{J}}{\mathrm{d}c} = -\frac{\partial \vec{F}}{\partial c}\vec{\xi}^* + \frac{\partial \mathcal{J}}{\partial c}, \tag{25}$$

so that imposing $\mathrm{d}\mathcal{J}/\mathrm{d}c = 0$ is equivalent to solving the optimality system (21).

Numerically, the condition $\mathrm{d}\mathcal{J}/\mathrm{d}c = 0$ is imposed by a method of steepest descent as

$$c^{(i+1)} = c^{(i)} - \alpha \frac{\mathrm{d}\mathcal{J}}{\mathrm{d}c}\Big]_{c^{(i)}}, \tag{26}$$

where i indicates the iteration number and α is a descent parameter to be determined. The algorithm is then the following:

0. The control variable is initialised with zero: $c = 0$;
1. The state variable u is determined from the state system (19);
2. The adjoint variables ξ_u and ξ_c are determined from the adjoint system (22);
3. $\mathrm{d}\mathcal{J}/\mathrm{d}c$ is calculated;
4. The control variable is updated using equation (26);
5. The process goes back to step 1 and iterates until convergence.

In our case, the constraints are given by equations (1), (2) and (4), $\vec{q}$ is the vector of state variables, $V_w(x)$ is the control variable and $\vec{\xi}$ is the vector of Lagrange multipliers (or receptivity coefficients). We have used two kinds of cost functional. The first is

$$\mathcal{J}(\vec{q}, V_w) = \frac{1}{2}\int_0^\infty u^2(x_{\text{fin}}, y)\,\mathrm{d}y + \frac{\gamma^2}{2}\int_{x_{\text{in}}}^{x_{\text{fin}}} {V_w}^2(x)\,\mathrm{d}x. \tag{27}$$

The second kind of cost functional used is

$$\mathcal{J}(\vec{q}, V_w) = \frac{1}{2}\int_{x_{\text{in}}}^{x_{\text{fin}}}\int_0^\infty u^2(x, y)\,\mathrm{d}y\,\mathrm{d}x + \frac{\gamma^2}{2}\int_{x_{\text{in}}}^{x_{\text{fin}}} {V_w}^2(x)\,\mathrm{d}x. \tag{28}$$

In both cases the parameter γ may be used to limit the 'size' of the control. However, there is another possibility to limit the size of this control, if necessary: it is quite simply to add a constraint of the type $\|V_w\| \leqslant K$. The velocity of blowing and suction is of the same order of magnitude as the normal component of the velocity of the disturbance, namely $Re^{-1/2}$. The control considered here is thus not a very expensive control, since the normal velocity at the wall is smaller than the longitudinal velocity of perturbation, and its cost was not taken into account in the objective functional to be minimised. That means taking $\gamma = 0$ in equation (27).

Thereafter, the lagrangian functional is defined as

$$\mathcal{L}(\vec{q}, V_w, \vec{\xi}, \zeta) = \mathcal{J}(\vec{q}, V_w) - \mathcal{D}(\vec{q}, \vec{\xi}) - \mathcal{C}(\vec{q}, V_w, \zeta), \tag{29}$$

where $\zeta(x)$ is the Lagrange multiplier representing the wall receptivity, and

$$\begin{aligned}
\mathcal{D}(\vec{q}, \vec{\xi}) &= \int_{x_{\text{in}}}^{x_{\text{fin}}}\int_0^\infty \vec{\xi}\cdot\left[\left(\underline{\underline{B}}\vec{q}\right)_x + \underline{\underline{A}}\vec{q}\right]\mathrm{d}y\,\mathrm{d}x,\\
\mathcal{C}(\vec{q}, V_w, \zeta) &= \int_{x_{\text{in}}}^{x_{\text{fin}}} \zeta(x)\cdot\big(v(x,0) - V_w(x)\big)\,\mathrm{d}x.
\end{aligned} \tag{30}$$

The adjoint equations can be determined from the extremality condition that

$$\delta\mathcal{L}_{\vec{q}} = \lim_{\varepsilon\to 0}\frac{\mathcal{L}(\vec{q} + \varepsilon\,\delta\vec{q}, V_w, \vec{\xi}, \zeta) - \mathcal{L}(\vec{q}, V_w, \vec{\xi}, \zeta)}{\varepsilon} = 0, \tag{31}$$

where $\delta\vec{q} = (\delta w, \delta p, \delta u, \delta v)^T$ is an arbitrary variation of $\vec{q}$. We then find equations (9) again, with the following conditions

$$\begin{aligned}
&b(x,0) = c(x,0) = d(x,0) = 0,\\
&a(x,0) + c_y(x,0) = \zeta,\\
&a(x,\infty) + c_y(x,\infty) + 2c(x,\infty)V(x,\infty) = 0,\\
&\overline{u}(x_{\text{fin}}, y) = u(x_{\text{fin}}, y),\\
&\overline{\eta}(x_{\text{fin}}, y) = 0,
\end{aligned} \tag{32}$$

which include both the boundary conditions (10) and the initial conditions (at the 'final' x) for the parabolised adjoint problem.

The optimality condition is

$$\gamma^2 V_w + \zeta = 0, \tag{33}$$

which for $\gamma = 0$ yields $\zeta = 0$. This condition is implicitly imposed by our iterative method, which means that 0 is the asymptotic value towards which the wall receptivity ζ tends during the iterative process (cf. second equation of the system (32)).

When the cost functional (28) is chosen, the system (32) becomes slightly different from (9), because there appears a forcing term in the first equation:

$$a_x + Ub_x + Vc_x + (Vb)_y + b_{yy} - \beta^2 b - 2G^2 Uc = u. \tag{34}$$

3.2. Input/output formulation

The result of the numerical integration of the forward system can be formally expressed without loss of generality in an input/output formulation:

$$u_{\text{out}} = \underline{\underline{U}} u_{\text{in}} + \underline{\underline{K}} V_w. \tag{35}$$

In this formulation, u_{out} is the downstream response, u_{in} is the initial perturbation, and V_w is the blowing and suction at the wall (the control). $\underline{\underline{U}}$ and $\underline{\underline{K}}$ are linear operators that transform the input perturbation and the control into the output response. In our case, the input perturbation u_{in} has been fixed to be the optimal perturbation calculated in [9] (see *figure 2*), whereas the control has been optimised so as to minimise the output.

The definitions of input and output energy appropriate to the boundary layer, which take into account the different scalings of longitudinal and transverse velocity, were also taken from Luchini [9], and adopted with no modification here:

$$E_{\text{in}} = \left[\int_0^\infty \left(|v|^2 + |w|^2\right) \mathrm{d}y\right]_{x=x_{\text{in}}} \quad \text{and} \quad E_{\text{out}} = \left[\int_0^\infty |u|^2 \,\mathrm{d}y\right]_{x=x_{\text{out}}}. \tag{36}$$

The definition of the energy of the control is

$$E_c = \int_{x_{\text{in}}}^{x_{\text{out}}} |V_w|^2 \,\mathrm{d}x, \tag{37}$$

whence we define a norm of the control as

$$\|V_w\| = \sqrt{E_c}. \tag{38}$$

We have considered two kinds of optimisation.

First, we have minimised the energy of the disturbance at the output cross-section only (cost functional (27)). To find this type of optimal control means to minimise E_{out}. We write that

$$\left|u_{\text{out}}\right|^2 = \left(\underline{\underline{U}} u_{\text{in}} + \underline{\underline{K}} V_w\right)^* \cdot \left(\underline{\underline{U}} u_{\text{in}} + \underline{\underline{K}} V_w\right), \tag{39}$$

where the sign * indicates complex conjugation.

So, minimisation of E_{out} requires that $\mathrm{d}E_{\text{out}}/\mathrm{d}V_w = 0$ (cf. section 3.1), that is to say

$$\underline{\underline{K}}^{T*} \cdot \left(\underline{\underline{U}} u_{\text{in}} + \underline{\underline{K}} V_w\right) = 0. \tag{40}$$

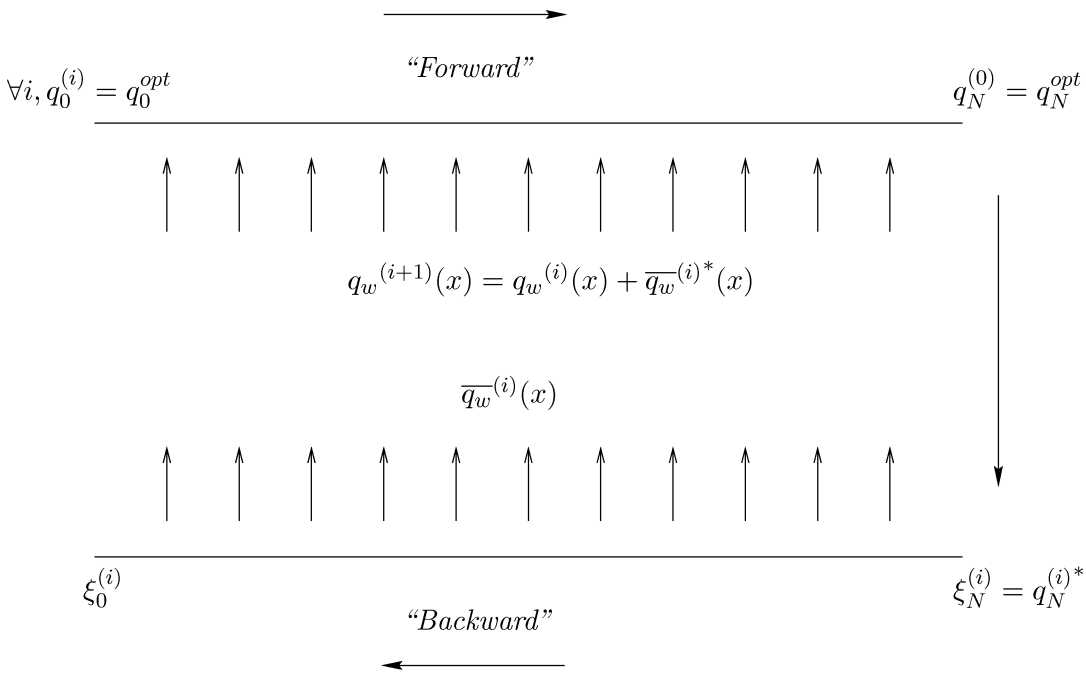

Figure 1. Practical determination of the optimal control by a minimisation of the downstream energy.

Albeit more sophisticated iterations could be devised, an algorithm of the form

$$V_w^{(i+1)} = V_w^{(i)} - \underline{\underline{K}}^{T*} \cdot (\underline{\underline{U}} u_{\text{in}} + \underline{\underline{K}} V_w{}^{(i)}) \tag{41}$$

already converges to the optimal control by blowing/suction at the wall, V_w, that corresponds to the minimal E_{out}.

We have also made calculations in which we required the energy of blowing/suction at the wall to be limited by a given value E_{c0}. In this case, we modify the algorithm (after the given value is exceeded) into

$$V_w^{(i+1)} = \frac{\underline{\underline{K}}^{T*} \cdot (\underline{\underline{U}} u_{\text{in}} + \underline{\underline{K}} V_w{}^{(i)})}{\|\underline{\underline{K}}^{T*} \cdot (\underline{\underline{U}} u_{\text{in}} + \underline{\underline{K}} V_w{}^{(i)})\|} \cdot \sqrt{E_{c0}}. \tag{42}$$

The second kind of optimisation is based on the minimisation of the longitudinal mean of the energy of the disturbance (cost functional (28)). In this case, we want to minimise $\int_0^L E_{\text{out}} \, \mathrm{d}x_{\text{out}}$. The algorithm is similar to the previous one, but with a different adjoint operator $\underline{\underline{K}}^{T*}$.

We must stress that the introduction of the operators $\underline{\underline{U}}$, $\underline{\underline{K}}$ and $\underline{\underline{K}}^{T*}$ is purely formal, and we never need to compute a matrix representation of these operators. Rather, $(\underline{\underline{U}} u_{\text{in}} + \underline{\underline{K}} V_w)$ is obtained at each step as the numerical solution of the forward problem with initial condition u_{in} and wall condition V_w, and $\underline{\underline{K}}^{T*} \cdot (\underline{\underline{U}} u_{\text{in}} + \underline{\underline{K}} V_w)$ is obtained at each step as the numerical solution of the backward problem with initial condition $(\underline{\underline{U}} u_{\text{in}} + \underline{\underline{K}} V_w)$ at the output station.

3.3. Iterative algorithm

In order to determine the optimal control, we have used a forward/backward algorithm. The scheme in *figure 1* summarises the numerical determination of the optimal mode of blowing/suction in the case of the minimisation of the downstream energy (first case). The superscript ^{i} indicates the number of 'forward-backward marches' performed. The superscript $^{\mathrm{opt}}$ indicates the optimal perturbation or the optimal mode. Finally, we use the superscript * to indicate complex conjugation.

In practice, we initialise the first backward march by $\overline{u}^{0} = \delta u^{*\mathrm{opt}}$ and $\overline{\eta}^{0} = 0$. Then, for each following backward march, we initialise by $\overline{u}^{i} = \delta u^{*i}$ and $\overline{\eta}^{i} = 0$ (cf. the last two equations (32)). During the backward march, for each station x we determine the wall receptivity according as

$$\overline{q}_{w}^{i}(x) = \left(\vec{\xi}_{n_x} + \vec{\xi}_{n_x}^{(1)}\right) \cdot \underline{\underline{B_{n_x}}} \cdot \underline{\underline{T_{n_x}}}^{-1} \cdot \underline{C_{n_x}}\Big|^{i}, \tag{43}$$

in which $n_x = x/\Delta x$, and $\underline{\underline{T_n}} = \underline{\underline{A_n}} + 1/\Delta x \underline{\underline{B_n}}$ at first order (see equations (16)) or $\underline{\underline{T_n}} = \underline{\underline{A_n}} + 1.5/\Delta x \underline{\underline{B_n}}$ at second order (see equations (18)).

Then, we initialise the blowing/suction velocity at the wall for the next forward march as

$$\vec{q}_{w}^{\,i+1}(x) = \vec{q}_{w}^{\,i}(x) + \overline{q}_{w}^{*i}(x). \tag{44}$$

We use the same kind of procedure to determine the optimal control in the case of the minimisation of the mean energy, except that during the backward march we also use the result of the previous forward march at each station in x as a forcing term; cf. equation (34).

For the next step, the blowing and suction velocity at the wall is re-initialised as

$$\vec{q}_{w}^{\,i+1}(x) = \vec{q}_{w}^{\,i}(x) + \frac{1}{N+1-n_x}\overline{q}_{w}^{*i}(x), \tag{45}$$

and we start again.

4. Results

4.1. Minimisation of the downstream energy

As a first case, we considered a flat-plate boundary layer. *Figures 2*(*a*) and (*b*) show the profiles of v and w representing an optimal perturbation, for three different values of the wavenumber β, and *figure 2*(*c*) shows the corresponding perturbation of longitudinal velocity produced at the outlet. We may note that $\beta = 0.45 \cdot \delta^{-1}$ is the wavenumber of maximum amplification (see Luchini [9]). Therefore, many results of this paper have been computed for this particular value of β. The energy of the input perturbation has been normalised to 1. The iterative algorithm has been stopped at a residual $\varepsilon = 10^{-5}$.

First, we have calculated the optimal blowing and suction at the wall (in this case the one that minimises the downstream energy of the longitudinal velocity perturbation) for three values of wavenumber ($\beta = 0.25 \cdot \delta^{-1}$, $\beta = 0.45 \cdot \delta^{-1}$ and $\beta = 0.65 \cdot \delta^{-1}$). The result is plotted in *figure 3*. We notice that the largest difference between the three wavenumbers is observed at the beginning ($0 \leqslant x \leqslant 0.2 \cdot L$) of the flat plate, where the blowing is strongest. This behaviour indicates that the neighbourhood of the leading edge is the most sensitive region of receptivity. This optimal control changes alternatively its direction along the wall (i.e., it consists of

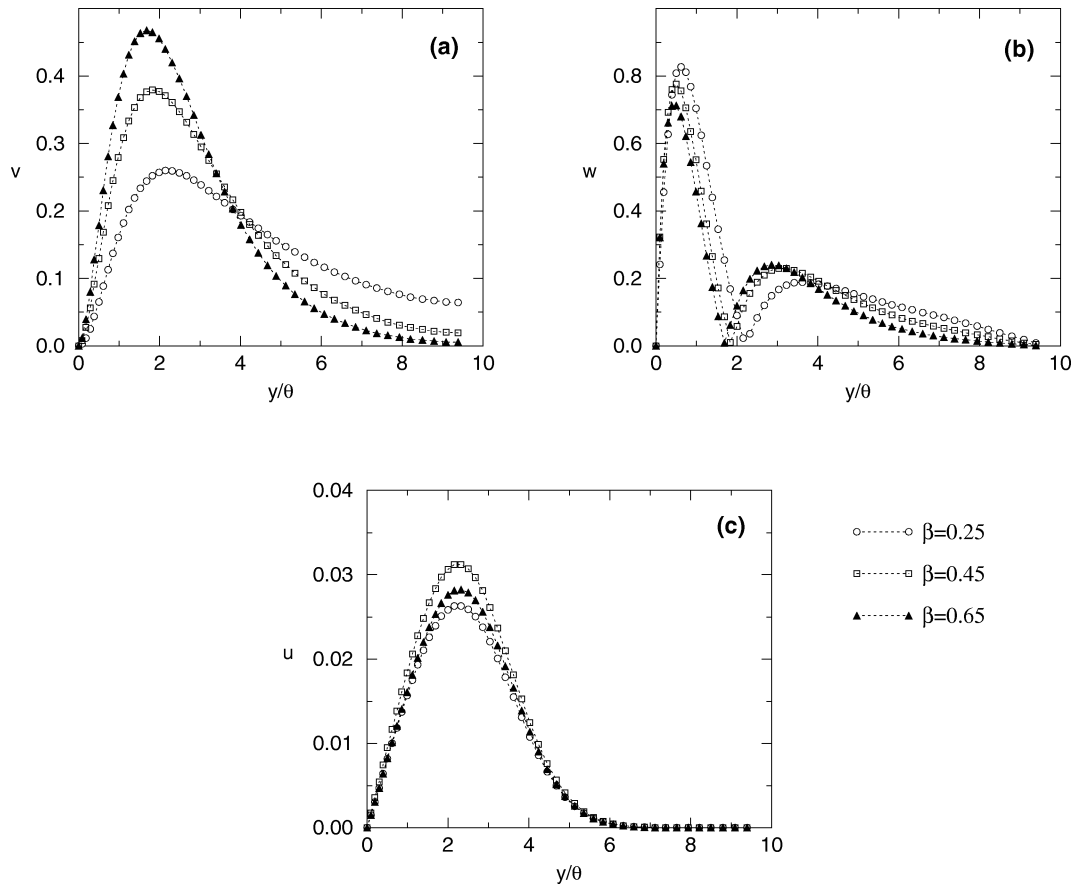

Figure 2. Profile of the (a) normal and (b) transverse velocity of the optimal perturbation of the flat plate boundary layer. (c) Profile of the final longitudinal velocity of perturbation induced by this optimal perturbation.

a succession of regions where blowing and suction are opposite in phase. It should be remembered that all disturbances considered here are oscillating in the z-direction, so that positive and negative swoops of the plot do not correspond to regions of exclusive blowing or suction but just to a change in the phase of the oscillation). The dimensionless energy of the control, E_c, equals 0.0304 for $\beta = 0.25 \cdot \delta^{-1}$, 0.0548 for $\beta = 0.45 \cdot \delta^{-1}$, and 0.0816 for $\beta = 0.65 \cdot \delta^{-1}$. These values, however, have turned out to be somewhat sensitive to the numerical discretisation adopted because of the difficulty in representing the final rapidly oscillating part properly. Of course, this rapid oscillation would also pose practical realization problems, and indeed we shall later present other solutions which do not exhibit this oscillation nor the related numerical difficulties. *Figure 4* displays the profile of the longitudinal velocity perturbation at $x = x_{\text{out}}$ before and after application of the control, for $\beta = 0.45 \cdot \delta^{-1}$. We can notice that the optimal control can indeed annihilate the output perturbation completely. However, whereas the energy at the output is reduced all the way to zero, the energy at intermediate stations (particularly just before $x \approx 0.6 \cdot L$) becomes considerably bigger than in the case without control (see *figure 5*). This behaviour indicates that in practice the control might produce an effect opposite to the one desired. Indeed, the control thus applied strongly modifies the energy of the transverse disturbance since very near the input station (see *figure 6*). As a consequence, the growth of longitudinal energy occurs earlier and quicker than in the case without control.

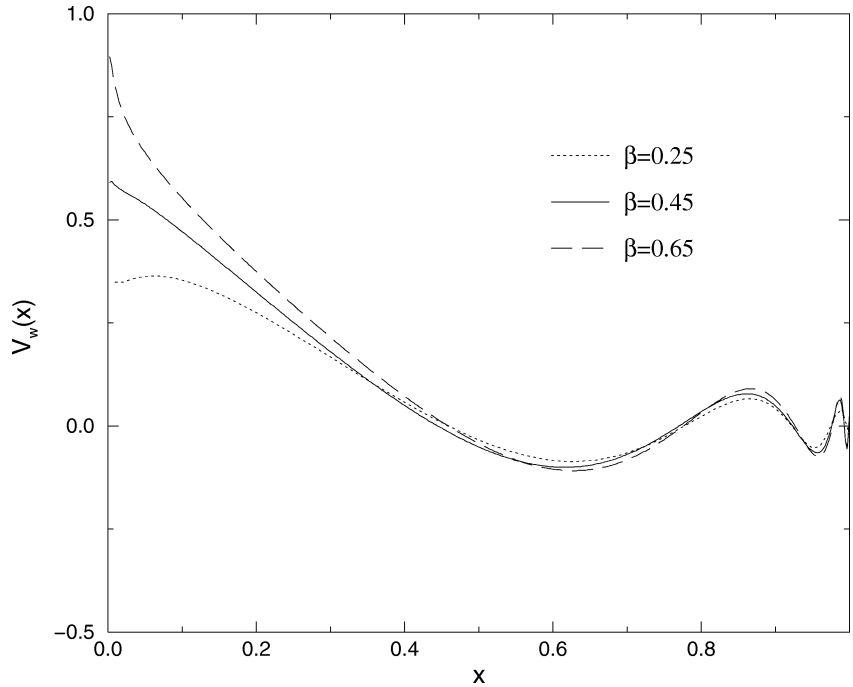

Figure 3. Profile of the optimal blowing and suction at the wall (flat plate).

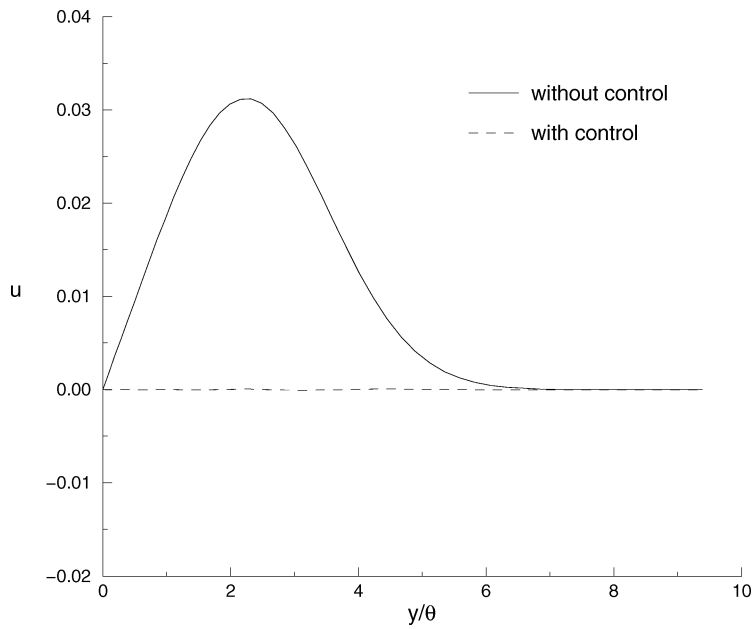

Figure 4. Profile of the longitudinal velocity at $x = L^{-1}$ with and without control at the wall (flat plate; $\beta = 0.45 \cdot \delta^{-1}$).

In a second attempt we kept a bound on the energy (cost) of the control, and at the same time on the kick given to the flow near the inlet, by modifying our problem into a constrained optimisation and the iterative algorithm into equation (42); of course this meant accepting a minimal but nonzero energy at the output. We

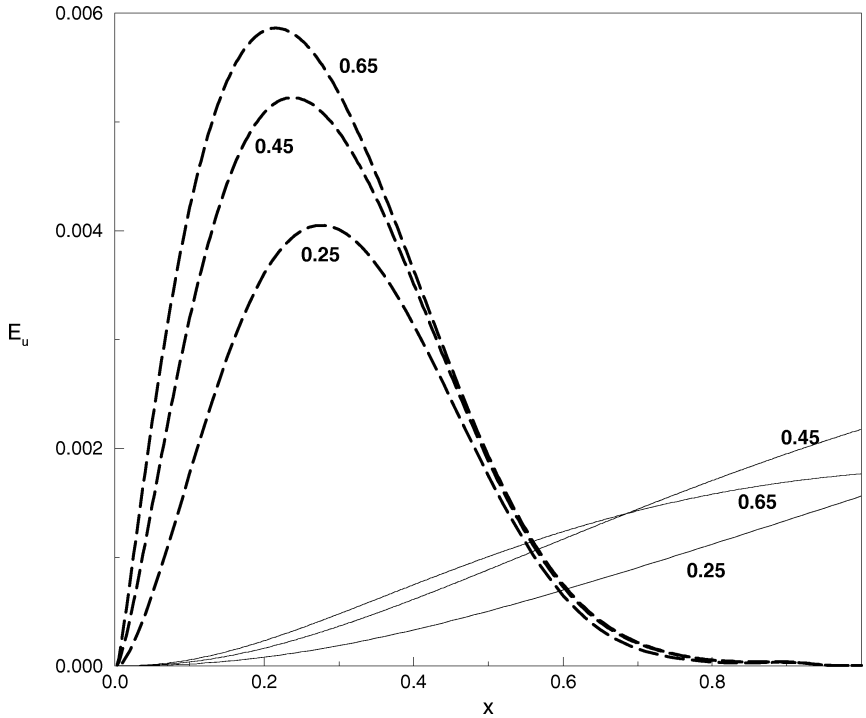

Figure 5. Streamwise evolution of the u-energy (flat plate).

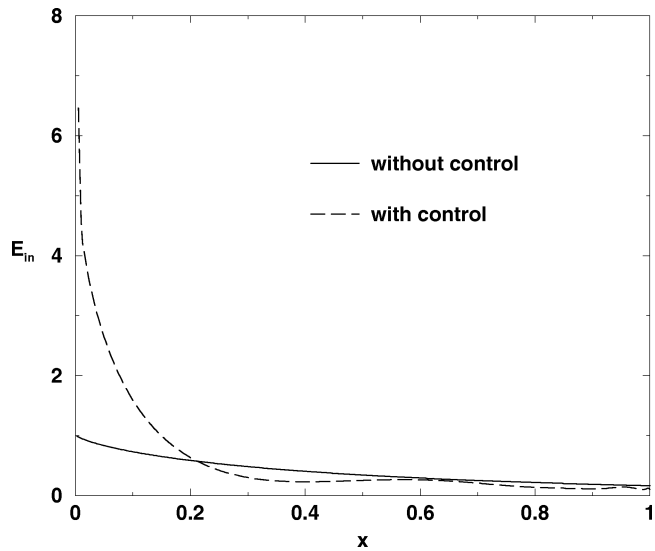

Figure 6. Streamwise evolution of E_{in} (flat plate; $\beta = 0.45 \cdot \delta^{-1}$).

imposed four values of maximum control energy: $E_c = 0.005$, $E_c = 0.01$, $E_c = 0.02$, and $E_c = 0.03$. *Figure 7* presents the different profiles of blowing and suction obtained. We notice that the more the energy is limited the more the control is 'uniform' (i.e., tends to keep a constant direction along the wall). The downstream responses to these controls are plotted in *figure 8*. The lower E_c is, the less the downstream E_u is minimised, and the less

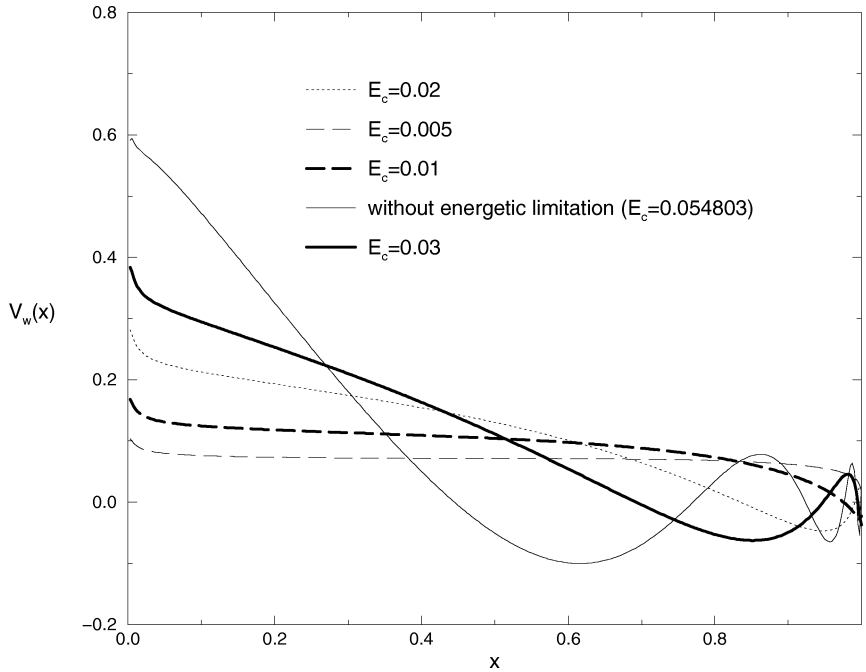

Figure 7. Profile of the blowing and suction at the wall with an energetic limitation (flat plate; $\beta = 0.45 \cdot \delta^{-1}$).

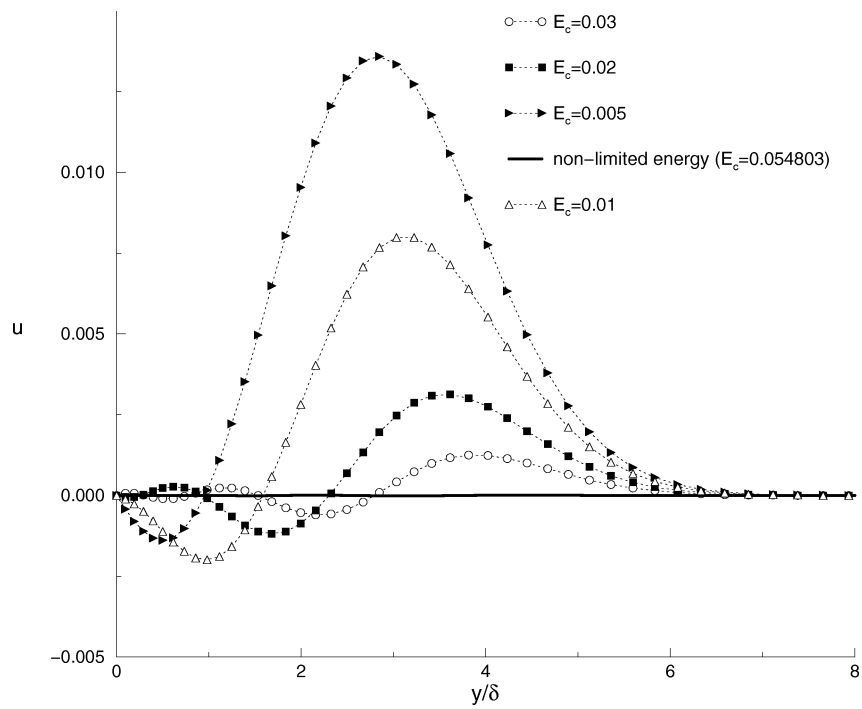

Figure 8. Profile of the longitudinal velocity at $x = L^{-1}$ with an energetic limitation (flat plate; $\beta = 0.45 \cdot \delta^{-1}$).

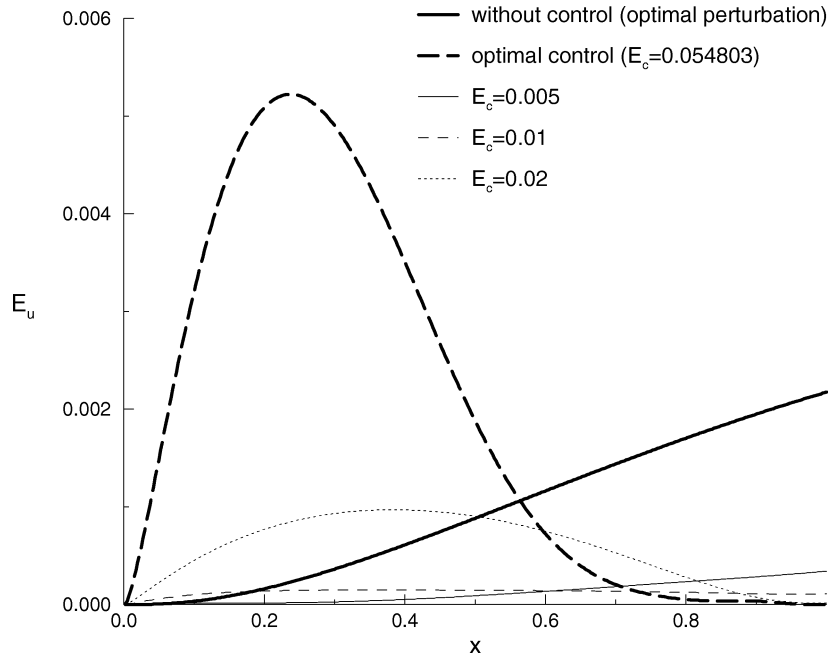

Figure 9. Streamwise evolution of the u-energy with an energetic limitation (flat plate; $\beta = 0.45 \cdot \delta^{-1}$).

the shape of the Klebanoff mode is altered. However, the u-energy now evolves very differently upstream, and a very significant reduction can be achieved everywhere with respect to the uncontrolled case (see *figure 9*). So, a control with its dimensionless energy limited to, say, 0.005 could be more effective in practice than one with unlimited energy.

Next, we considered the case of a concave wall. *Figure 10* shows the optimal control for $G_\theta = 0$ (flat plate), $G_\theta = 10$, and $G_\theta = 20$. For the case of $G_\theta = 10$ the optimal control changes direction three times along the wall. For the case of $G_\theta = 20$ the optimal control does not change its direction at all, and in fact is practically different from zero only between $x = 0$ and $x \approx 0.77 \cdot L$. This means that the receptivity region becomes more and more concentrated near the leading edge with increasing wall curvature. We can compare this behaviour of receptivity at the leading edge with the results obtained by Luchini and Bottaro [28] on Görtler's instability. Indeed, they found that the receptivity to wall disturbances is maximum at the leading edge. *Figure 11* shows the final u profile (on a very enlarged scale), and the streamwise evolution of E_u is plotted in *figure 12*. We notice that the sharp energy increase observed near the inlet in the case of a flat plate tends to disappear with increasing curvature of the wall. Thus, for sufficiently large curvatures, this form of blowing-and-suction control can be effective.

4.2. Minimisation of the mean energy

In a third attempt, we have performed calculations in which we minimised the streamwise mean energy of the longitudinal perturbation (using equation (34)). First, we calculated the optimal blowing and suction at the wall in the case of a flat plate, and for three values of the wavenumber β ($\beta = 0.25 \cdot \delta^{-1}$, $\beta = 0.45 \cdot \delta^{-1}$, and $\beta = 0.65 \cdot \delta^{-1}$). The results are plotted in *figure 13*(*a*), whereas the evolution of the longitudinal energy E_u can be seen in *figure 13*(*b*). We can observe that this type of optimisation gives more interesting results than the previous one. Indeed, although the output energy is not completely damped, energy is now everywhere

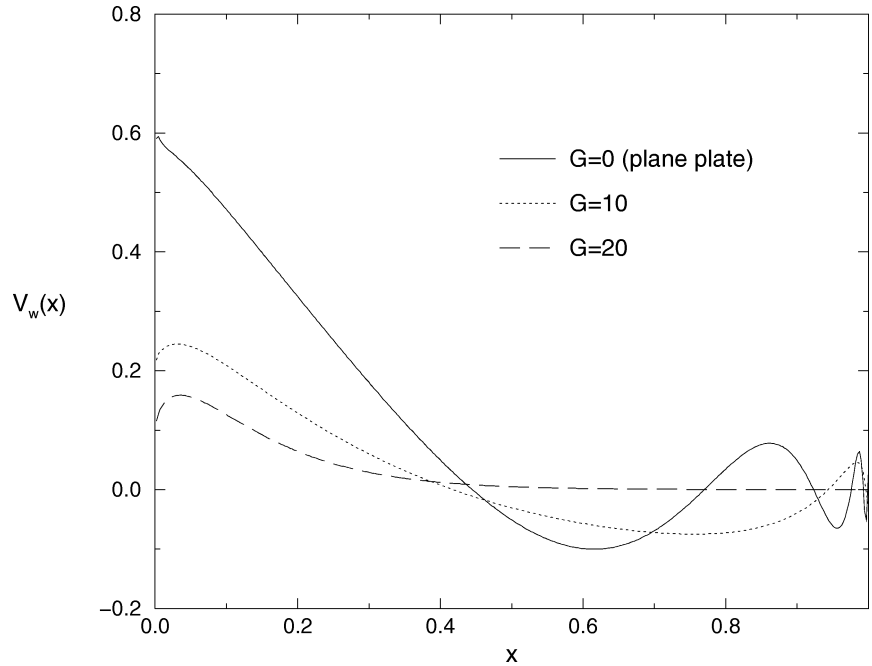

Figure 10. Profile of the optimal blowing and suction at the wall for a curved wall ($\beta = 0.45 \cdot \delta^{-1}$).

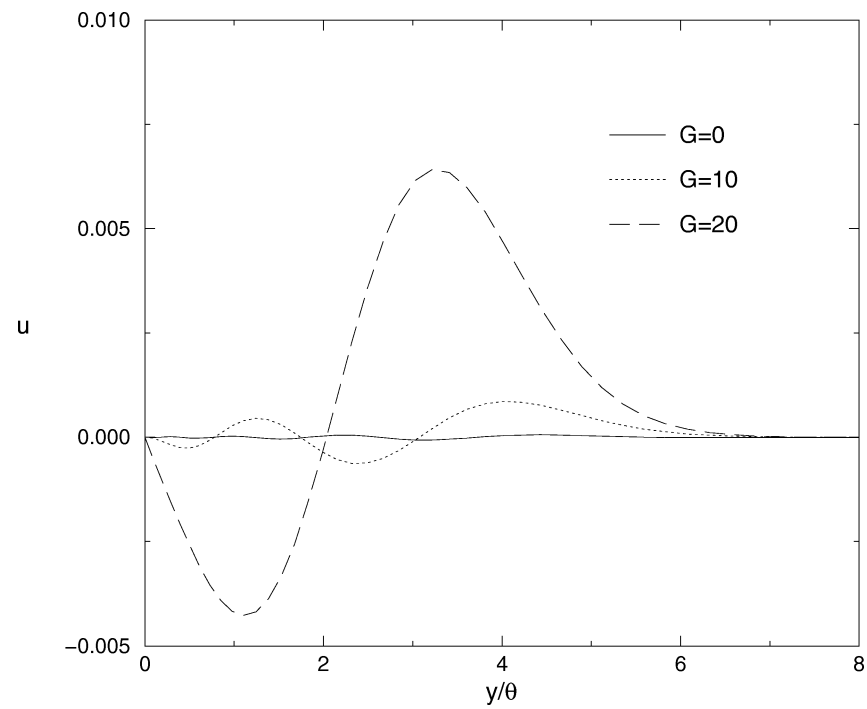

Figure 11. Profile of the final longitudinal velocity for a curved wall ($\beta = 0.45 \cdot \delta^{-1}$).

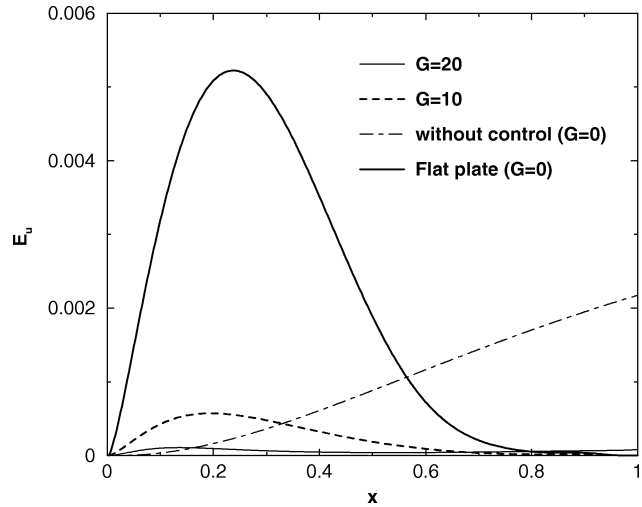

Figure 12. Streamwise evolution of the u-energy for a curved wall ($\beta = 0.45 \cdot \delta^{-1}$).

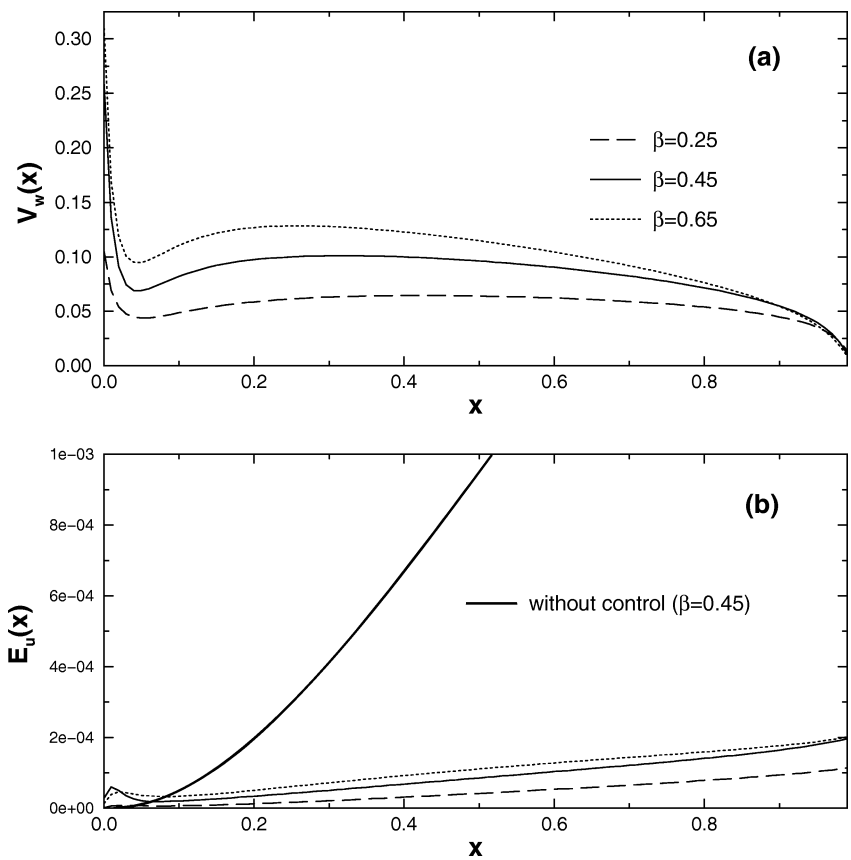

Figure 13. Minimisation of the longitudinal mean energy. (a) Profile of the optimal blowing and suction at the wall (flat plate). (b) Evolution of the u-energy.

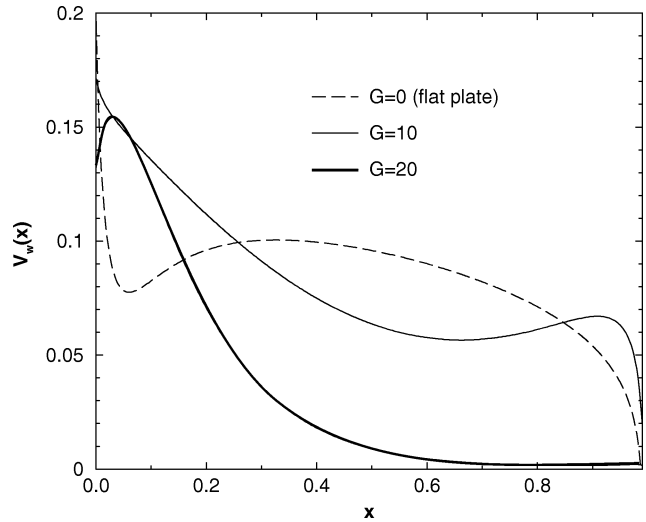

Figure 14. Minimisation of the longitudinal mean energy. Profile of the optimal $V_w(x)$ for three different Görtler numbers ($G = 0$, $G = 10$ and $G = 20$).

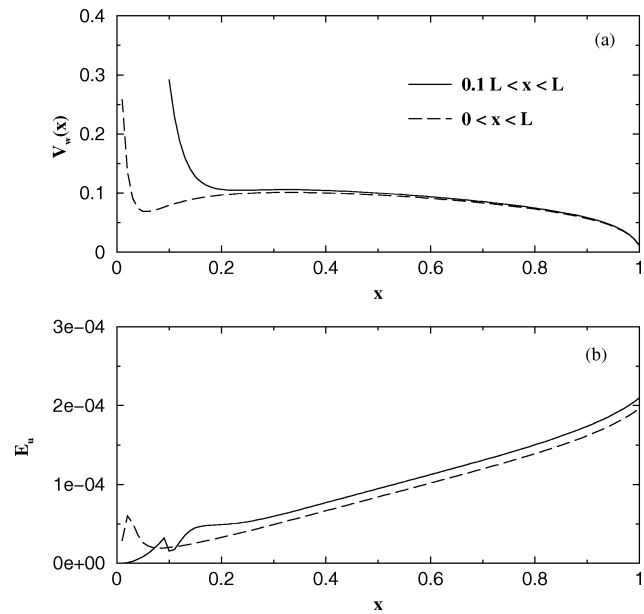

Figure 15. Minimisation of the longitudinal mean energy. Restriction of the domain of control to $0.1L < x < L$ (flat plate). (a) Profile of the optimal $V_w(x)$. (b) Evolution of the u-energy E_u.

strongly reduced with respect to the uncontrolled case. The shape of the control is also one-signed and much more regular (and easier to realize), with only one sharp peak at the inlet, which is consistent with the previous observation that the strongest receptivity occurs at the leading edge of the plate.

For a curved plate, *figure 14*(*a*) shows the profile of $V_w(x)$ for three values of the Görtler number, $G = 0$, $G = 10$ and $G = 20$. The more significant the curvature of the wall, the less the difference between the two types of optimisation. This behaviour implies that in the case of a very concave wall the minimisation of the mean or the downstream energy gives more or less equivalent results.

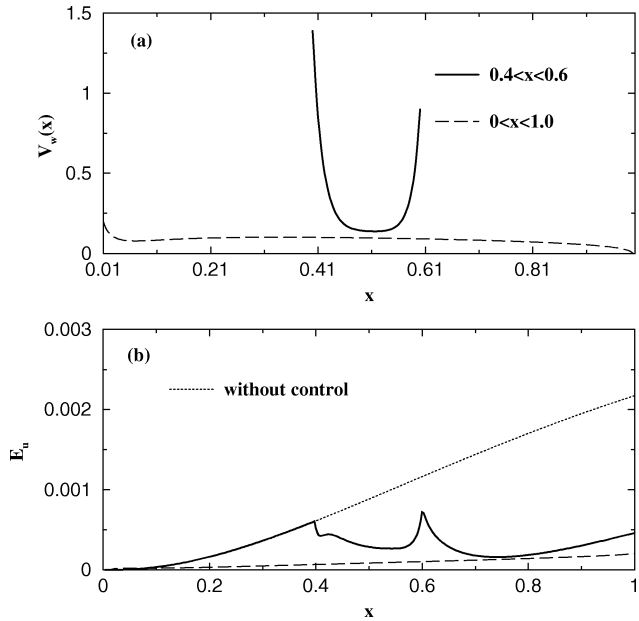

Figure 16. Minimisation of the longitudinal mean energy. Restriction of the domain of control to $0.4L < x < 0.6L$ (flat plate). (a) Profile of the optimal $V_w(x)$. (b) Evolution of the u-energy E_u.

Since creating a very large blowing or suction near the leading edge may be practically difficult, in a further set of tests we have limited the spatial extent of the control to see how much its effectiveness becomes degraded if the initial region is excluded. In a first run, the blowing/suction is only present for $x > 0.1L$. The optimal $V_w(x)$ thus found is plotted in *figure 15*(*a*), and the corresponding evolution of the disturbance energy in *figure 15*(*b*). In a second, more severely constrained, optimisation, we have reduced the range of application of the control to $0.4L < x < 0.6L$. The results are plotted in *figures 16*(*a*) and (*b*).

In both cases we can notice that a significant reduction is still achieved, and in addition the control does not change sign along the wall. This feature implies that it could be technically easier to perform such a control.

5. Conclusions

The aim of this paper was a numerical determination of a control by blowing and suction at the wall of the optimal perturbations of the boundary layer. We have searched for an optimal control at the wall using a receptivity approach. We have found the optimal profile of this blowing and suction in both cases of a flat and of a curved wall. The region near the leading edge is where the wall receptivity is highest (particularly for the curved plates). By trying different optimisation criteria, we have shown that a very significant reduction of the disturbance energy can be achieved, but attention must be paid not to increase the energy at intermediate stations when seeking to minimise it at the output.

Acknowledgements

This work was started when the first author was a visitor at the Politecnico di Milano and continued in the Institut de Mécanique des Fluides de Toulouse. Professor A. Bottaro is thanked for useful comments and discussions.

References

[1] Landahl M.T., A note on a algebraic instability of inviscid parallel shear flows, J. Fluid Mech. 98 (1980) 243–251.
[2] Hultgren L.S., Gustavsson L.H., Algebraic growth of disturbances in a laminar boundary layer, Phys. Fluids 24 (1981) 1000–1004.
[3] Gustavsson L.H., Energy growth of three-dimensional disturbances in plane Poiseuille flow, J. Fluid Mech. 224 (1991) 241.
[4] Butler K.M., Farrell B.F., Three-dimensional optimal perturbation in viscous shear flow, Phys. Fluids A 4 (1992) 1637.
[5] Henningson D.S., Lundbladh A., Johansson A.V., A mechanism for bypass transition from localised disturbances in wall-bounded shear flows, J. Fluid Mech. 250 (1993) 169–207.
[6] Reddy S.C., Henningson D.S., Energy growth in viscous channel flow, J. Fluid Mech. 252 (1993) 57–70.
[7] Trefethen L.N., Trefethen A.E., Reddy S.C., Driscoll T.A., Hydrodynamic stability without eigenvalues, Science 261 (1983) 578–584.
[8] Luchini P., Reynolds-number-independent instability of the boundary layer over a flat surface, J. Fluid Mech. 327 (1996) 101–115.
[9] Luchini P., Reynolds-number-independent instability of the boundary layer over a flat surface: optimal perturbations, J. Fluid Mech. 404 (2000) 289–309.
[10] Andersson P., Berggren M., Henningson D., Optimal disturbances in boundary layer, in: Borggaard J.T., Burns J., Cliff E., Schreck S. (Eds.), Proc. AFOSR Workshop on Optimal Design and Control, Arlington VA, USA, 30 Sept.–3 Oct. 1997, Birkhäuser, Boston, 1998.
[11] Andersson P., Berggren M., Henningson D., Optimal disturbances in boundary layer, Phys. Fluids 11 (1999) 134–150.
[12] Klebanoff P.S., Tidstrom K.D., Sargent L.M., The three-dimensional nature of boundary layer instability, J. Fluid Mech. 12 (1962) 1–34.
[13] Görtler H., Über eine dreidimensionale Instabilität laminaer Grenzschichten an Konkaven Wänden, Nachr. Ges. Göttingen, Math. Phys. Klasse, Neue Folge 2 (1940) 1–26.
[14] Hall P., Taylor–Görtler vortices in fully-developed flows or boundary layers: linear theory, J. Fluid Mech. 124 (1982) 475–494.
[15] Hall P., The linear development of Görtler vortices in growing boundary layers, J. Fluid Mech. 130 (1983) 41–58.
[16] Floryan J.M., Saric W.S., Stability of Görtler vortices in boundary layers, AIAA J. 20 (1982) 316–324.
[17] Swearingen J.D., Blackwelder R.F., The growth and breakdown of streamwise vortices in the presence of a wall, J. Fluid Mech. 182 (1987).
[18] Peerhossaini H., Wesfreid J.E., On the inner structure of streamwise Görtler rolls, Int. J. Heat Fluid Fl. 9 (1) (1988) 12–18.
[19] Sabry A.S., Liu J.T.C., Longitudinal vorticity elements in boundary layers: nonlinear development from initial Görtler vortices as a prototype problem, J. Fluid Mech. 231 (1991).
[20] Saric W.S., Görtler vortices, Annu. Rev. Fluid Mech. 26 (1994).
[21] Bottaro A., Klingmann B.G.B., On the linear breakdown of Görtler vortices, Eur. J. Mech. B-Fluids 15 (3) (1996).
[22] Kendall J.M., Experimental study of disturbances produced in a pre-transitional laminar boundary layer by weak freestream turbulence, AIAA Paper 85 (1985) 1695.
[23] Anders J.B., Blackwelder R.F., Longitudinal vortices in a transitioning boundary layer, IUTAM 1979, Laminar – Turbulent Transition, Springer-Verlag, 1979.
[24] Floryan J.M., Saric W.S., Stability of Görtler vortices in boundary layers with suction, AIAA 12-th Fluid and Plasma Dynamics Conf. Williamsburg, AIAA Paper 79-1479, 1979.
[25] Myose R.Y., Blackwelder R.F., Control the spacing of streamwise vortices on concave walls, AIAA J. 29 (11) (1991) 1901–1905.
[26] Myose R.Y., Blackwelder R.F., Control of streamwise vortices using selective suction, AIAA J. 33 (1995) 1073–1080.
[27] Hill D.C., Adjoint systems and role in the receptivity problem for boundary layers, J. Fluid Mech. 292 (1995) 183.
[28] Luchini P., Bottaro A., Görtler vortices: a backward-in-time approach to the receptivity problem, J. Fluid Mech. 363 (1998) 1–23.
[29] Gunzburger M., Flow Control, Springer, Berlin, 1995.
[30] Borggaard J., Burkardt J., Gunzburger M., Peterson J., Optimal Design and Control, Birkhäuser, Boston, 1995.
[31] Bewley T.M., Moin P., Temam R., Optimal and robust approaches for linear and nonlinear regulation problems in fluid mechanics, AIAA Paper No 97-1872, 1997.
[32] Bewley T.R., Temam R., Ziane M., A general framework for robust control in fluid mechanics, Physica D (1999) (submitted).
[33] Gunzburger M., Hou L., Finite dimensional approximation of a class of constrained nonlinear optimal control problems, SIAM J. Control Optim. 34 (1996) 1001–1043.
[34] Abergel F., Temam R., On some control problems in fluid mechanics, Theor. Comp. Fluid Dyn. 1 (1990) 303–325.
[35] Moin P., Bewley T.R., Feedback control of turbulence, Appl. Mech. Rev. 47 (6) part 2 (1994).
[36] Temam R., Bewley T.R., Moin P., Control of turbulent flows, Proc. 18th IFIP TC7, System Modelling and Optimisation, Detroit, Michigan, July, 1997.
[37] Joslin R.D., Gunzburger M.D., Nicolaides R.A., Erlebacher G., Hussaini M.Y., A self-contained, automated methodology for optimal flow control, AIAA J. 35 (1997) 816–824.

[38] Joshi S.S., Speyer J.L., Kim J., A systems theory approach to the feedback stabilization of infinitesimal and finite-amplitude disturbances in plane Poiseuille flow, J. Fluid Mech. 332 (1997) 157–184.
[39] Bewley T.R., Liu S., Optimal and robust control and estimation of linear paths to transition, J. Fluid Mech. 365 (1998) 305–349.
[40] Gunzburger M., Inverse design and optimisation methods: Lagrange multiplier techniques, Von Karman Institute for Fluid Dynamics, Lecture Series 1997-05, April, 1997.